

United States Hydrographic Conference 2015

March 16th-19th

National Harbor, Maryland, USA

Multispectral Acoustic Backscatter from Multibeam, Improved Classification Potential

John E. Hughes Clarke

Abstract

Most multibeams today provide a measure of the received seabed backscatter intensity. With proper radiometric and geometric reduction, the seabed backscatter strength and its angular variation may be derived, which can then be used to attempt seabed classification. Most multibeams, however, are monochromatic in the sense that they transmit using a single center frequency (even if with some pulse bandwidth). The seabed scattering is thus specific to that wavelength. As a result ambiguities in classification can result when differing scattering mechanisms (e.g. surface and volume) result in a similar intensity at that wavelength.

If, in contrast, the seabed can be imaged using a triplet of discrete center frequencies, each spaced about an octave apart, the frequency dependence may be used as an additional classifier. Additional complications exist, however, with the added requirement to perform those same corrections, but now for three different systems. A major concern is the proper accounting for path length attenuation for the highest frequency involved, as that limits the maximum depth over which the combined systems can be used.

Multispectral imaging has been implemented twice now using co-located 70-100 kHz and 200-400 kHz multibeams. Examples of improved seabed discrimination are presented. Clear variations in the shape of the angular response curve as well as the relative scattering between frequencies are demonstrated.

Biographical Notes

John E. Hughes Clarke is the Chair in Ocean Mapping and a Professor in the Department of Geodesy and Geomatics Engineering at UNB. His prime interest lies in submarine sediment transport processes. As part of this, maximizing the information content available from integrated swath sonar systems is a major component of his research.

Contact Details

John E. Hughes Clarke
Tel. +1 (506) 453-4568
Fax +1 (506) 453-4943
E-mail: jhc@omg.unb.ca

Dept. Geodesy and Geomatics Engineering
University of New Brunswick
P.O. Box 4400
Fredericton, NB, E3B 5A3, CANADA

Multispectral Acoustic Backscatter from Multibeam, Improved Classification Potential

John E. Hughes Clarke

Ocean Mapping Group, Dept. Geodesy and Geomatics Engineering, University of New Brunswick, P.O. Box 4400, Fredericton, NB, E3B 5A3, Canada

jhc@omg.unb.ca

Abstract

Most multibeams today provide a measure of the received seabed backscatter intensity. With proper radiometric and geometric reduction, the seabed backscatter strength and its angular variation may be derived, which can then be used to attempt seabed classification. Most multibeams, however, are monochromatic in the sense that they transmit using a single center frequency (even if with some pulse bandwidth). The seabed scattering is thus specific to that wavelength. As a result ambiguities in classification can result when differing scattering mechanisms (e.g. surface and volume) result in a similar intensity at that wavelength.

If, in contrast, the seabed can be imaged using a triplet of discrete center frequencies, each spaced about an octave apart, the frequency dependence may be used as an additional classifier. Additional complications exist, however, with the added requirement to perform those same corrections, but now for three different systems. A major concern is the proper accounting for path length attenuation for the highest frequency involved, as that limits the maximum depth over which the combined systems can be used.

Multispectral imaging has been implemented twice now using co-located 70-100 kHz and 200-400 kHz multibeams. Examples of improved seabed discrimination are presented. Clear variations in the shape of the angular response curve as well as the relative scattering between frequencies are demonstrated.

The Idea

Multibeam sonar systems have come to dominate the world of marine survey. Seabed topographic delineation is the core capability, but seabed backscatter strength mapping and water column volume imaging have grown as parallel deliverables. To meet the competing needs of range performance versus resolution, however, these systems have generally been narrow-band, providing scattering strength estimates only within ~ 10% of the center frequency. As a result the seabed and volume scattering products are essentially monochromatic. Scattering phenomena, however, can be strongly wavelength dependent (Ogilvy, 1991) and thus the benefits of multispectral imaging, so common in passive electromagnetic systems (colour) and active multi-frequency radar (van Zyl et al., 1991) are not yet routinely available to the marine survey community.

Recent advances in transducer technology and the need for wider bandwidths to achieve multiple sectors has expanded available bandwidth up to ~ 30-50% of center frequency. That bandwidth, however, is more commonly employed in achieving better range resolution and thus not available to be exploited for multi-spectral imaging. Ideally such multispectral imaging would benefit from yet broader frequency separation. This paper presents two examples of employing

paired sets of multibeams, thereby utilizing wavelengths separated by more than an octave. The challenges here are to work within the limitation of the attenuation constraints of the highest frequency and to properly reduce both datasets so that the multispectral signature will be free of sonar-specific radiation, geometric and environmental overprints.

Monospectral Backscatter Classification

At the heart of this approach is the desire to improve seafloor discrimination through the analysis of acoustic backscatter over a range of wavelengths. With the currently available monochromatic backscatter data, three main approaches have been taken: textural (Pace and Gao, 1982), angular response (deMoustier and Alexandrou, 1991, Hughes Clarke, 1994) and mean level (normalized for angular response, Hammerstad, 1995, 2000). In more recent developments, the three have been combined (Preston, 2009)

All these approaches however, have limitations. The textural approach, which is least sensitive to absolute calibration, is strongly dependent on pulse length used and is least useful at high grazing angles. The angular response requires very precise geometric and radiometric corrections, but appears to be most useful at those high grazing angles. The mean response can, at least in a relative sense, be used most broadly but generally is least useful at the near normal incidence region. But for all three, the classification can only work on the scattering response as observed at the center frequencies utilized. For a single sonar center frequency (typically dictated by the depth range) reasonable discrimination can usually be achieved but often ambiguities remain as quite different material types may exhibit near identical backscatter strength values over a limited range of grazing angles. Without utilizing much heavier survey overlap (e.g. Hughes Clarke, 1994), an alternate approach may be to use differing frequencies.

The Potential Advantages of Multispectral Classification

By recording backscatter strength and its angular response over widely changing wavelengths, two effects are expected. Firstly the relative roughness with respect to the wavelength may be different (depending on the exponent of the roughness spectrum). Secondly there is the potential for volume scattering in low impedance sediments to increase because of the lower sediment attenuation at longer wavelengths (Ryan and Flood 1996).

Early studies on the frequency dependence of scattering (NDRC, 1946, Urick, 1954) determined that there was little discernable dependence for very rough seabeds, but that the scattering appeared to increase with increasing frequency for softer seabeds. This frequency dependence is also predicted by the model described by Jackson et al. (1986) which predicted a 1.5 to 3dB increase per octave. Notably however, all these observations were conducted for frequencies between 10 and 80 kHz. Similarly the underlying assumptions in the model are questionable above 100 kHz. This study is contrast is looking at frequencies significantly above that level as those are the most suitable to meet the range/resolution requirements for coastal and continental shelf surveying.

Previous Work:

NRDC (1946) is probably the first example of looking at back scattering as a function of wavelength. Whilst using lower frequencies, their conclusion was that the observed variation in scattering strength between frequencies was smaller than their uncertainty in absolute calibration

of the sensors. This limitation of absolute calibration continues today as, to achieve this wide range of wavelengths, invariably multiple separate sensors are required, each of which has their own calibration uncertainty.

The idea of imaging using two or more co-mounted arrays has a long history in sidescan development. Search sidescans commonly are available in two channels, a “high frequency channel (commonly ~ 300-500 kHz) and a low frequency channel (commonly around 100 kHz). The two were not originally routinely used simultaneously, the low frequency being employed at longer ranges for regional reconnaissance and the higher frequency used at shorter ranges for detailed search. However, a number of companies allowed the option of utilizing both simultaneously.

The only published attempt to utilize this capability for the purpose of improved seafloor classification is Ryan and Flood (1996). They utilize two different configurations, a deep-towed sidescan system using 30 and 70 kHz center frequencies and a shallow water 100 and 500 kHz sidescan (a Klein 595). They clearly illustrated contrasting responses for certain sediment types which, for the lower frequency pair, they attributed to the relative depth of penetration and associated volume scattering. To make this comparison, they used the mean scattering level, avoided the near-nadir high grazing angle data and limited the coverage to the lesser of the two swaths. If this approach can be replicated with multibeam sonar, with their ability to better account for the geometric changes at high grazing angles, this approach could be improved.

More recently this approach has been extended to the multibeam geometry. In an example where use of differing center frequencies has overlapped, it has been demonstrated (Hughes Clarke et al., 2008) that the response can vary significantly with wavelength and that the amount of contrast is sediment type dependent. If this extra degree of freedom can be incorporated, it could significantly improve discrimination. This is the core hypothesis of this approach.

Most recently, Imagenex are now offering a three frequency sidescan sonar (120,260,540 kHz) that combines those channels as a RGB pseudo-colour image (Imagenex, 2014). No results or analysis have yet been published however. As it is a sidescan geometry, probably only the low grazing angle region will be considered. Nevertheless, full radiometric and geometric correction will be required.

The Implementation - Multiple Sonars

Obtaining two octaves (factor of 4) variation in wavelength is not practical given the typical usable transducer bandwidth in a single multibeam system. The available coastal and continental shelf sonars on the market today generally fall into two classes: the 200-400 kHz range (R2Sonic 2022/4, RESON 7125 and EM2040) and the 70-100 kHz range (RESON 7111 and EM710). So only by combining these can one cover the required range of wavelengths. To test this concept, combined low and high frequency multibeams were mounted on the same vessel. The systems used were an EM710 for the 70-100 kHz, range and EM2040 for the 200-400 kHz range. The configuration was attempted twice on two different platforms.

The first configuration was undertaken on board USNS Mary Sears, a 100m ocean going survey vessel belonging to the U.S. Naval Oceanographic Office. The 0.5°x1.0° version of the EM710

was used together with the $0.5^\circ \times 1.0^\circ$ version of the EM2040S. The two were located several metres apart on a gondola mounted $\sim 7\text{m}$ below the water line.

The second configuration was undertaken on board CSL Heron, a 10m coastal survey launch operated by the Ocean Mapping Group at UNB. A $1.0^\circ \times 2.0^\circ$ version of the EM710 was used together with the $\sim 1.3^\circ \times 1.3^\circ$ EM2040C. The 710 was on a small gondola and the 2040C was located ~ 2 metres away in a keel blister.

While the two versions of the EM710's use identical pulse lengths, sectors and swath spacings, the two versions of the EM2040 differ. The full EM2040S, uses 3 discrete sectors across track for 300 and 400 kHz (2 for 200kHz) over two swaths (6 discrete transmissions per shot cycle). The EM2040C, however, only has a single sector and a single swath and thus only transmits once using a single centre frequency. The EM2040C at 400 kHz is restricted to a $+/-40^\circ$ sector and thus was not usable for these tests. As the 2040C has only one transmission, greater bandwidth is available and thus shorter pulses are used than the 2040S which requires 4 discrete bandwidths to serve the 4 or 6 sectors. As a result the 2040S did not change its pulse length during these surveys unlike the 2040C which was continually changing the pulse length.

Unfortunately, the EM2040 can only operate in one of its 3 frequency bands at a time. Thus, in the first pass, the seafloor was imaged simultaneously using the EM710 at 70-100 kHz and the EM2040 centered at 300 kHz. To complete the coverage, the survey had to be rerun at 200 kHz and, (if utilized), again at 400 kHz. A significant future improvement for the 2040 would be to be able to use the dual swath to acquire data at two of the frequency settings simultaneously.

Data Manipulations Steps:

If the frequency and grazing angle variation in backscatter strength is to be used as a classifier, the logged data have to be adequately reduced for radiometric and geometric effects. There are several steps that have to be applied to the data that are described in turn below.

In order to get at the backscatter strength measurement, the observed intensity needs to be reduced for all of the source level (and its angular variations), the receiver sensitivity (and their angular variations), applied gains, the ensonified area and transmission losses.

Getting back to the observed Intensity:

Some manufacturers directly log a measure of that received intensity that just subsequently requires reduction for the above-listed parameters. Other manufacturers, specifically Kongsberg Maritime (KM), whose data are used in this work, attempt an approximation of the data reduction before logging. In addition to the factors listed above, the KM data reduction method (Hammerstad, 2000) utilizes a simplified model of the grazing angle variation to attempt to provide normalized data. Thus before utilizing logged KM data, the applied grazing angle correction, as well as the simplifying assumptions inherent in the applied ensonified area calculation, needs to be removed before reapplying the standard steps.

To remove these steps, the minimum slant range, the crossover angle and the estimate of the backscatter at normal incidence and oblique incidence (Hammerstad 2000) need to be extracted from the telegram and back corrected for. This has been done to the data herein, although there continues to be concerns about the details of this reduction.

The ensonified area calculation – grazing angle derivation and pulse length dependence.

To reduce to an estimate of the seabed backscatter strength, the received intensity has to be normalized for instantaneous ensonified area. This requires knowledge of all of the transmit and receive beamwidths, the pulse length and the local grazing angle (Urick, 1954).

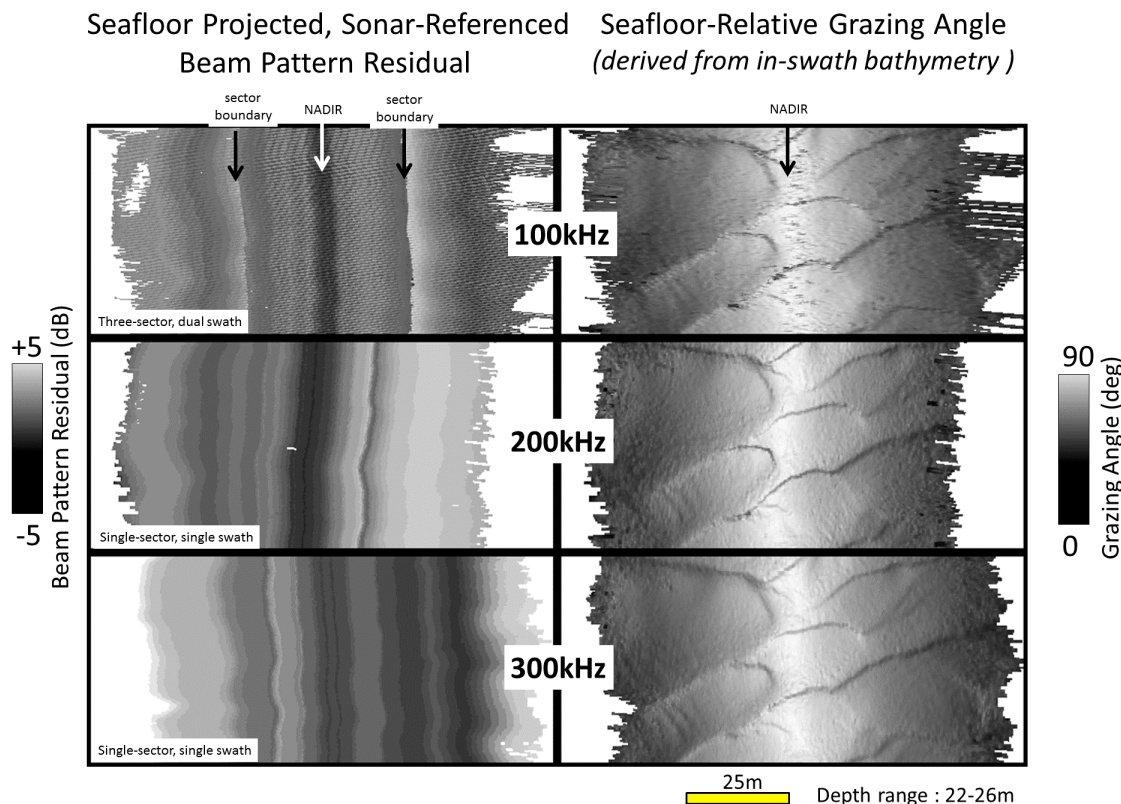


*Fig 1: Illustrating data reduction steps required to extract the seabed backscatter strength.
LEFT: Sonar-Relative Residual Beam Patterns RIGHT: Sea-floor Relative Grazing Angle
Note that the beam patterns are unique to each sonar and, for the case of the EM710, unique to each sector of each swath (6 in total). The beam patterns rotate as the sonar reference frame rolls. Those patterns for multiple sectors however, are truncated at the sector boundaries which are stabilized to be fixed in the vertical reference frame.*

Note also the variable quality of the grazing angle estimates based on the beam to beam bottom detection noise. The lower range resolution of the EM710 produces notably noisier slope estimates at nadir.

First the real-time ensonified area correction, which is based on a simplified model of a flat seafloor (Hammerstad, 2000) needs to be removed. This accounts for the utilized pulse length. Once removed an improved model of the ensonified area now needs to be applied. This is done using the pulse length, the transmit and receive beam width (which varies within a swath as the sector frequencies are shifted) and a more faithful estimate of the local grazing angle (Fig. 1 right). This estimate is obtained for each beam by fitting a 3D plane to the bottom detection solution and the 8 immediate detection neighbours. While imperfect due to sounding noise,

slopes over length scales of several beam spacings are well captured. The main limitations are tracking in the outer most beams and on the edge of shadows.

Figure 1 (right) illustrates the derivation of the local grazing angle from a swath of data over a rough (bedform covered) seafloor. As can be seen, the grazing angles range from normal incidence (90°) to beyond the designed angular sector ($\pm 65^\circ$ which would result in 25° grazing on a flat seafloor). As the seafloor is not flat, the grazing angles deviate from the simple real-time model. Notably, often true normal incidence is not actually sampled as most sonars run with transmitter tilted forward to avoid the specular echo. Also, because the seafloor is often tilted away from the sonar (for example the backside of dunes), grazing angles smaller than 25° may be obtained. Those data obtained closed to limiting grazing (e.g. the edge of a shadow) should, however, be treated with suspicion. Similarly at the outer edge of the swath, the spurious sounding noise can result in distorted grazing angle estimates leading to contaminated backscatter strength values at low grazing angles.

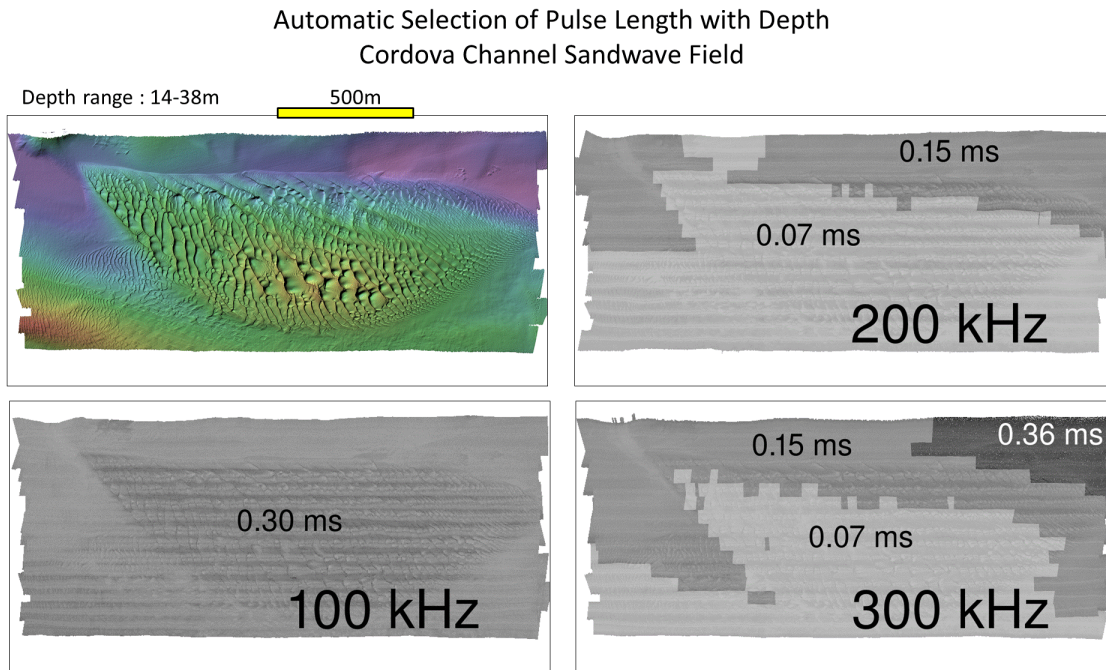


Fig 2: Showing the depth distribution in the Cordova Channel Sandwave field and the choice of pulse length used by the different multibeam configurations as the data were collected over the same areas. As can be seen, the pulse length is increased as function of water depth.

Away from normal incidence, as well as the grazing angle, the estimate of the ensonified area requires knowledge of the pulse length used. That is often operationally altered automatically to maintain sufficient signal to noise. This must be accounted for (Fig. 2).

For the case of the Cordova Channel data, in order to maintain optimal signal to noise, the 200 and 300 kHz modes of the EM2040C automatically adjusted the utilized pulse length as a function of depth. Figure 2 above illustrates the relationship of pulse length utilized and the water depth. The EM710, as it was not signal to noise limited, used its shortest available pulse length for the whole area.

For the Roberts Channel data, having learnt from the previous experience, the pulse length was fixed for the area. For the Saipan Reef survey, as the multi-sector and swath EM2040 was used, the default pulse length did not change over the depth range considered (24-38m).

Residual sonar-referenced beam patterns

Ideally each multibeam transmission would generate the same source level over the full range of elevation angles. In reality there is an across track variation in the intensity distribution of the transmitter. For a single sector system such as an EM2040C that corresponds to a single function in elevation from port to starboard in a sonar-referenced frame. For multi-sector systems such as the EM710 or full EM2040, there are three discrete sectors for each swath and two swaths in total. Thus up to 6 transmission functions need to be defined per mode. Various previous attempts have been developed to address the issue of multi-sector beam patterns (Llewellyn, 2005, Hughes Clarke, 2012, Teng 2012).

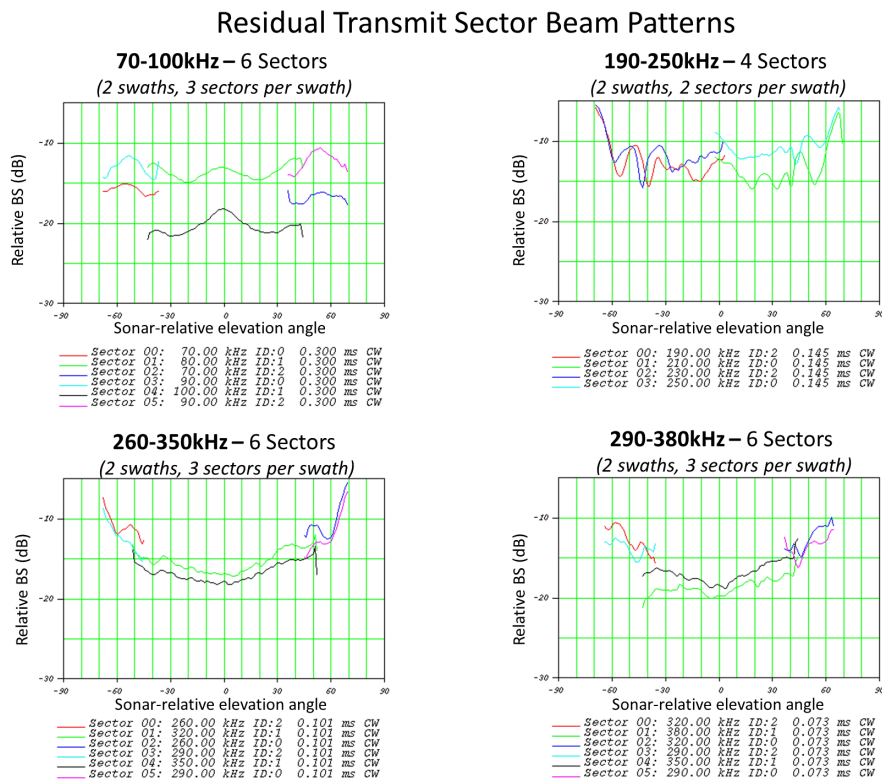


Fig 3: Showing the estimated residual transmit beam patterns for each of the 4 or 6 sectors used in the 4 different frequency ranges. The data were acquired over a common large patch of living coral whose response was assumed to be Lambertian. The data are with respect to the sonar reference frame, not the vertical.

Ideally these functions would be known from theoretical or test tank experiments. However, it is clear that these patterns vary from unit to unit even for nominally identical sonar models (Hughes Clarke et al., 2008). Thus a means of extracting these residual variations is required under field conditions. This can be problematic as the other reason that one might see variations in received intensity with elevation angle are the angular response of the seabed backscatter

strength. Thus one needs to know this apriori to extract the beam pattern variations. Of course usually that angular response is exactly what you are trying to measure.

The approach used herein is to collect data from an anomalously rough seafloor such as gravel pavements or living coral that is believed to exhibit a near predictable Lambertian scattering response. For each beam, the local grazing angle is calculated (Fig. 1 right) and the predicted scattering strength drop with respect to normal incidence is calculated. For that same beam the sonar relative angle and the associated sector characteristics are also extracted and the departure from an average level for each beam is compiled by stacking all beams at that instantaneous sonar-referenced angle.

The result of this stacking in the sonar reference frame is shown in figure 3. As can be seen there are either 6 or 4 individual functions corresponding to the sectors in the dual swath cycle. These reference residual patterns are then removed from all the data based on each beam's orientation with respect to the transmitter at transmit time. The resulting correction, if projected on the seafloor (Fig. 1 left) is seen to roll back and forth with the sonar. This correction is then subtracted from the observed data. This very effectively removes fluctuations of intensity unrelated to the seabed geology and grazing angle variation.

Absolute Source or Backscatter Level.

While the previous method removes elevation angle related variations in source level, it does not constrain the absolute source level as it is not clear which part (if any) of the transmission beam pattern is putting out the designed source level. Given the 5-10 dB variation in the apparent sonar-relative beam patterns, it is hard to be confident of the absolute scattering level or the offset between scattering at different frequencies. To do so would require that the absolute scattering level in the reference area be also known. All that can be strictly preserved is the change in relative scattering intensity between the three frequencies utilized. As will be demonstrated in the experimental results below, as well as changes in the relative shape of the angular response curves, the relative levels of scattering between the frequencies does notably alter with sediment type.

Varying Attenuation Coefficients

As part of the transmission losses, the path length attenuation over the slant range (out and back) has to be accounted for. That attenuation coefficient is a function of all of frequency, temperature, salinity and pressure (Francois and Garrison 1982). The table below illustrates the observed oceanographic conditions off Saipan and around the Gulf Islands in BC in February. For those conditions, the attenuation coefficient is calculated according to the three center frequencies utilized in these experiments.

Area	T °C	S ppt	100kHz α db/km	200kHz α db/km	300kHz α db/km
Saipan	27.5	34.7	35	88	127
BC in February	7.3	30.5	28	45	64

At these inner continental shelf depths a typical round trip slant range to an outermost beam is about 100m. Thus at ~ 100 kHz, the transmission loss would only vary between ~3 and 3.5 dB depending on the oceanography. The same path at 200 kHz, however, would incur a greater variation in signal loss of between ~5 and 9 dB and at 300 kHz, 6 and 13 dB. Thus clearly the local oceanographic conditions are required to prevent a bias in the data and this becomes more sensitive at the higher frequencies.

The resulting bias varies with slant range and thus would grow by grazing angle, distorting therefore, not only the absolute level but the slope of the apparent ARC. To mitigate this effect, Carvalho and Hughes Clarke, (2012) have directly addressed the method of correcting data in post-processing if the wrong oceanographic conditions are used in real time. Those corrections must take account of the varying frequencies within the multiple sectors of a single swath.

For the highest frequencies used, the high attenuation will result in the signal to noise level floor being approached for weak sediment and/or longest ranges. This could potentially contaminate estimates of seabed (and especially volume) scatter strength estimates. Thus a practical maximum range limit would have to be placed on the application of multispectral imaging, depending on the highest frequency chosen and the ambient noise levels. The examples used herein are all in depths less than 40m and are thus not affected by this issue.

Varying Grazing Angles

The resulting data is then a measure of the backscatter strength as a function of grazing angle herein referred to as the angular response curve (ARC). This in itself is a potential classifier (deMoustier, 1986, Hughes Clarke, et al., 1997, Fonseca and Mayer, 2007), but as normal surveys do not have heavy overlap, any spatial map can only provide one point on the curve for a given location. Thus most mosaic products attempt to normalize for the shape of the angular response. This is a necessary condition if the false colour composite method is to be applied to mosaicked products.

Most airborne and spaceborne electromagnetic techniques have the luxury of a high aspect ratio so that only a narrow range of elevation angles have to be utilized, thereby avoiding the need to compensate for the grazing angle dependence. As a result, where electromagnetic multi-spectral imaging is presented, the grazing angle dependence can be ignored or reduced using a simplified model. As, however, ship based acoustic imaging is constrained to a maximum elevation of the depth, a wider range of grazing angles is necessarily present in the data. As acoustic backscatter is strongly grazing angle dependent, it has always been a standard procedure to try and normalize this grazing angle variability by predicting the shape of the ARC. There are, however, two limiting criteria that make it extremely difficult to undertake that grazing angle normalization:

- 1 – the shape of the curve varies with lithology.
- 2 – for a single lithology, the shape varies with the frequency.

If one had the luxury of heavily overlapping imagery so that the range of grazing angles is reduced and/or a range of grazing angles for each location is available (e.g Hughes Clarke, 1994) the local variations in the shape of the ARC could be compensated for. Most surveys, however, require the use of data from normal incidence to at least 60 degrees incidence angle on both

sides. The three examples presented here were acquired with a typical operational survey mode using a +/-65° swath with only about 20% overlap.

Example Experimental Data

The Results – Saipan Reef

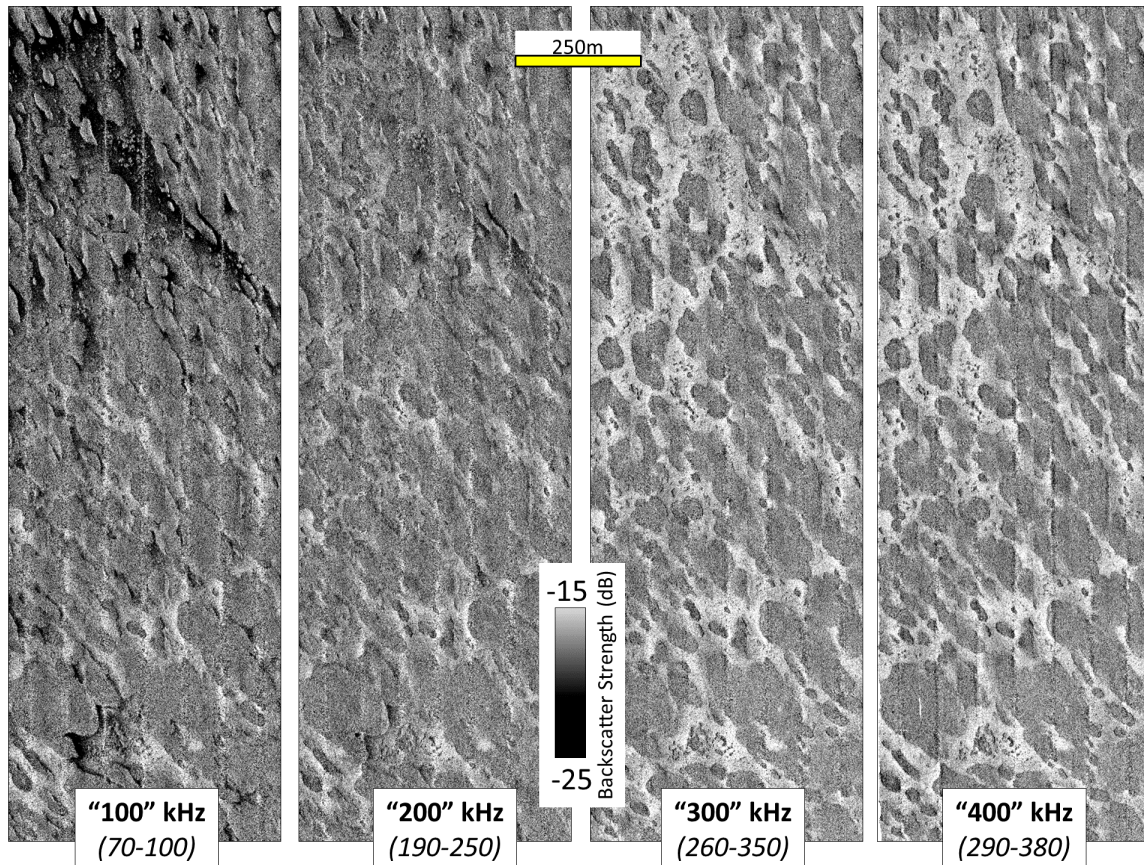


Fig 4: 1650m x 540m area of the Saipan Reef top, as viewed at 4 ranges of frequencies.

The first experiment was performed in April 2012 from USNS Mary Sears. Four frequency data were collected over alternating living coral and coral sand sheets on a current swept section of reef off Saipan in 25-40m of water. The data were reduced according to the steps outlined above. As can be seen from the multi-frequency mosaics presented in Figure 4, the spatial patterns seen in the mosaic are remarkably different at the different wavelengths. While the living coral appears very similar in scattering signature at all wavelengths, the scattering strength of the intervening unconsolidated coral sands varies both spatially and as a function of frequency.

At the low frequency end, the sand sheets appear to have two distinct facies with one that has a 5-7 dB lower signature than the coral (Fig 5, Low BS) and one that is ~3 dB higher than the living coral. As one moves up in frequency, most of that contrast disappears and the sand sheets now appear higher intensity than the living coral. At 200kHz, the contrast between the living coral and coral sand is minimal.

As can be seen, The 300 and 400 kHz imagery is almost identical in apparent spatial patterns (Fig 4 right) and angular response (Fig. 5 top left). This reflects the fact that, while the EM2040 is advertised as having a discrete mode at those two center frequencies, in order to accommodate the required bandwidth for the 6 sectors, the nominally 400 kHz data is in fact all below 400kHz and overlapping heavily with the range of frequencies used at the 300 kHz (which is truly centred around 300 kHz).

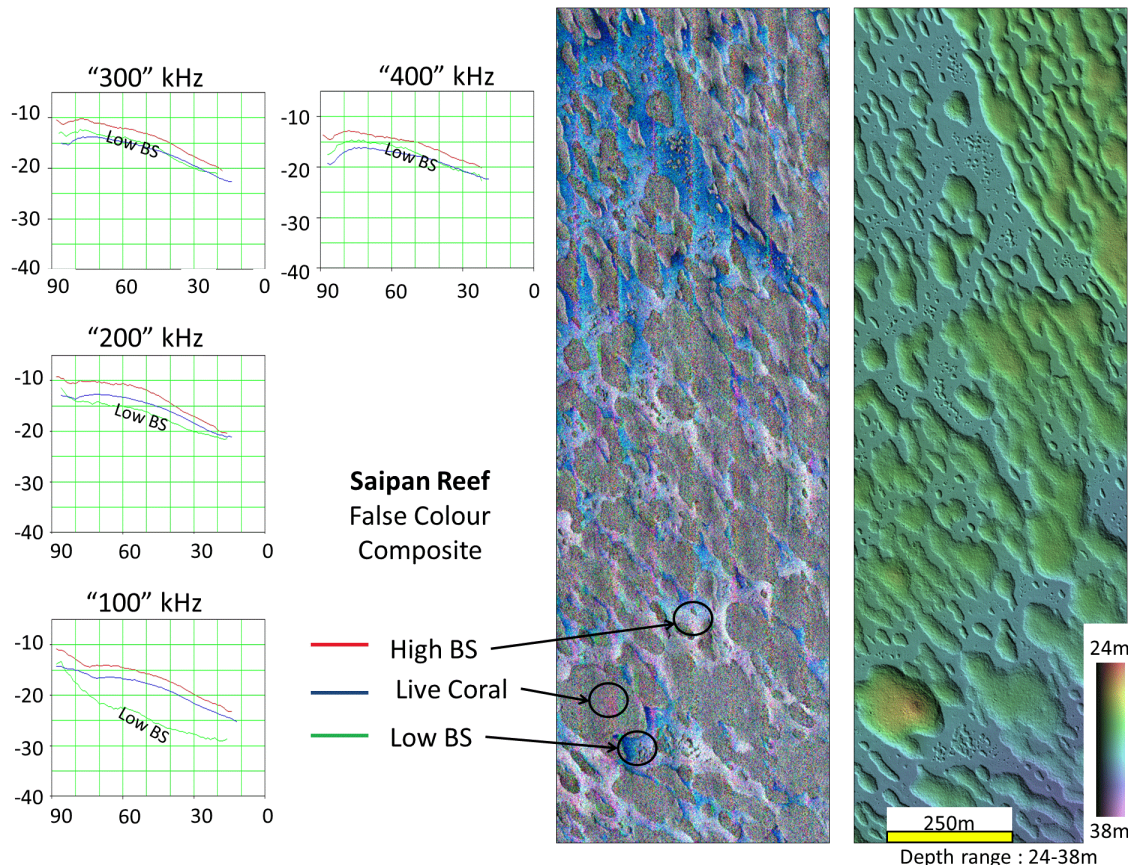


Fig 5 : Right – showing the same 1650m x 540m area of the Saipan Reef top as a false colour composite (RED- 100 kHz, GREEN, 200 kHz, blue, 300 kHz). And far right – the bathymetric terrain for the same area. Left – shows the reduced backscatter strength angular response curves for the three end member sediment types at the 4 frequency ranges utilized.

One can then take the nominal 100, 200 and 300 kHz imagery, all of which has been normalized for the average shape of the angular response, and compile them into a false colour composite (Fig 5 centre-right). As can be seen from representative ARCS extracted at the 4 different center frequencies (Fig. 5 left), apart from near nadir data at 100 kHz, the ARCS are almost parallel over the majority of the grazing angle range imaged. Thus the composite mosaics do not show pronounced along track striping.

As can be seen in the false colour composite, the living reef can be identified by a distinct colour and intensity (red tinge) reflecting the fact that its scattering strength decreases with increasing frequency. In contrast mobile coral sands exhibit two characteristics, one of which (the blue)

shows scattering strength increasing with frequency (Fig. 5 Low BS). The other part of the coral sand is high intensity at all three wavelengths and shows up as near white (Fig. 5 High BS).

The Results - Cordova Channel Dunefield

The second experiment was performed in February 2014 from the CSL Heron over actively migrating sand waves in the Cordova Channel in British Columbia (BC). The area is a tidally swept channel with trapped eddies developed off two headlands. In the eddy location, a banner bank has been developed in which continuously migrating coarse sand bedforms are present. The surrounding higher backscatter area is assumed to be a current swept gravel pavement.

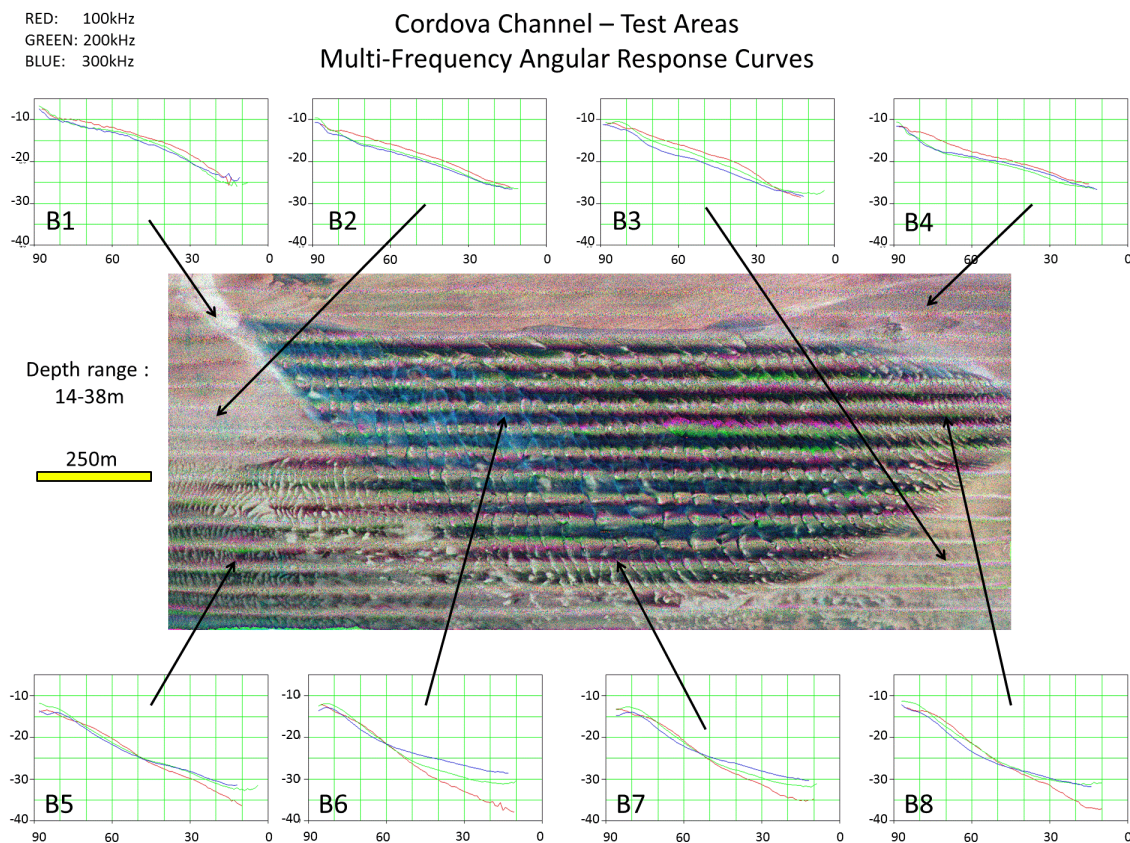


Fig 6: selected multispectral backscatter angular response curves from the Cordova Channel area. The top curves (B1-4) represent deflated gravel rich surfaces. The bottom curves (B5-8) represent mobile coarse sand moulded into bedforms.

The data were reduced using the steps described above and a mosaic was made in which the grazing angle compensation used only the ARC of one of the gravel areas (B2). Thus, as can be seen in Fig. 6, the grazing angle dependence is barely visible in those areas. In contrast to the gravel areas, the mobile sand has a much steeper ARC and thus much of the grazing angle variation remains in the mosaic.

In figure 6 on the top, four representative multi-frequency angular response curves are shown for the bedform free areas. For all, the roll off as a function of grazing angle is quite flat and close to Lambertian and areas B1-2-3 lack a strong near-specular peak. The higher scatter level and the shape of the ARC for B1-2-3 would suggest rougher higher impedance sediments. While the absolute level of scattering varies from area to area, there is little variation with frequency away from near nadir and thus the false colour image appears predominantly monochrome. This is in accordance with previous multi-spectral results (NRDC, 1946, Urick, 1954) that suggested little frequency dependence for rougher seabeds.

The lower scattering strengths in B4 do correspond with a more pronounced specular peak near nadir. The width and the height of the specular peak for B4 is seen to change with wavelength. Somewhat counter intuitively, though, the specular peak is least developed for the longest wavelengths.

On the bottom of Fig. 6 are four representative multi-spectral ARC's from the mobile coarse sand bedforms. They all exhibit a much steeper roll off with grazing angle and a more pronounced specular peak. Also at the lower grazing angles they all show decreasing scattering strength with longer wavelengths. Again this frequency dependence is in accordance with the softer sediment results of Urick, 1954).

Interestingly, for the sandy ARCS (B5-6-7-8), the amount of frequency dependence at the lowest grazing angles is quite variable amongst the sand wave field. At grazing angles above $\sim 60^\circ$, however, there is little frequency dependence. This may be a reflection of scattering dominated by volume contributions inside the critical angle (assuming a coarse sand sound speed of 1650-1750m/s the critical angle would lie in the $65\text{-}55^\circ$ range). Outside the critical angle, surface roughness dominates and thus this may be controlling the variations. Seabed type B6 shows the most frequency dependence and material with this characteristic stands out as a clearly defined bluer zone in the false colour composite.

The Results – Roberts Point

The third area again utilized the second configuration (CSL Heron in February 2014) and examines a current swept area in which no bedforms are developed. Fig. 7 shows the RGB composite of the area. The angular response was suppressed using the shape of the higher backscatter region (specifically site R2).

The three ARCS plots to the left of Fig. 7 illustrate the response over the high backscatter material all of which appear Lambertian and do not exhibit a notable near-specular peak (thus assumed to be rough gravels). On the right of Fig. 7, the ARC's of the lower backscatter sediments are presented (assumed to be sand sheets). As the shape of the angular response curve, especially towards normal incidence, is much more pronounced for R4-5-6, a strong nadir stripe appears and disappears in the mosaic as a function the changing seabed.

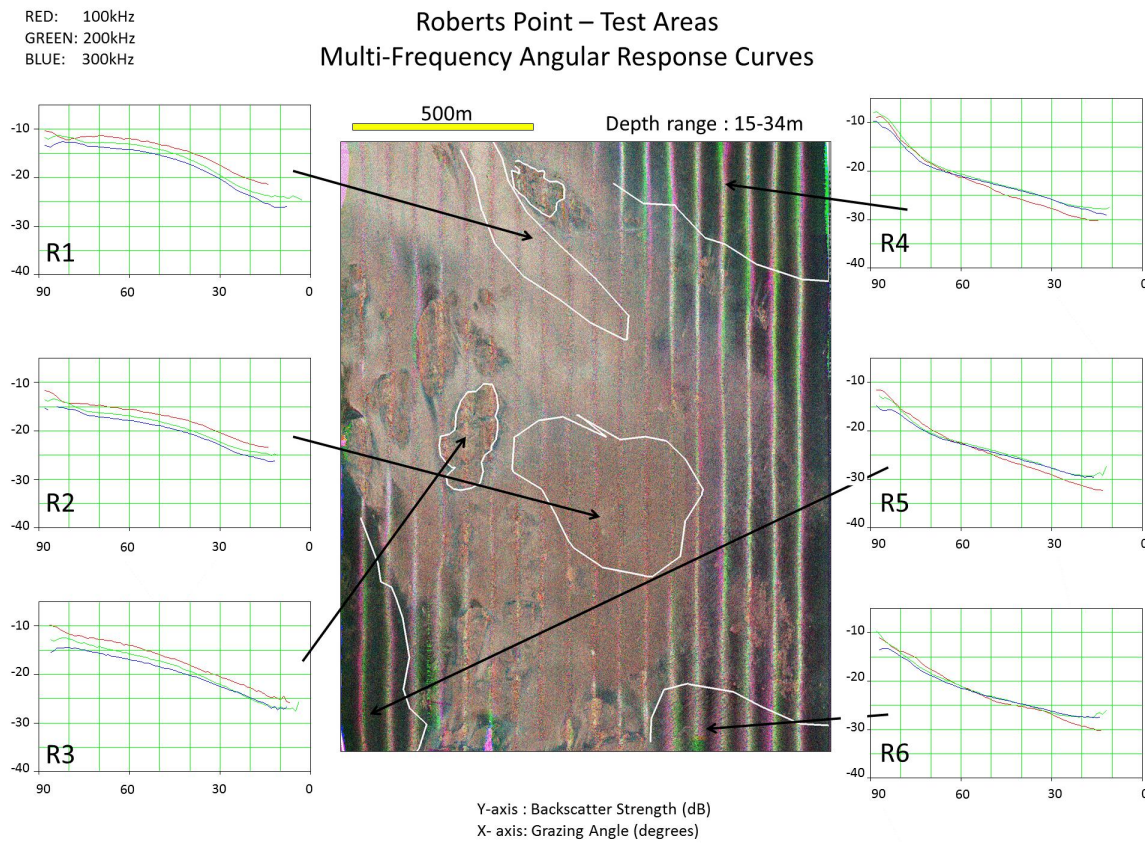


Fig 7: Centre: RGB composite mosaic of the Roberts Point test area (depth range 15-34m). Selected multispectral backscatter angular response curves are shown for the outlined areas. Curves to the left represent higher backscatter gravel and bedrock areas. Curves to the right represent lower backscatter finer sediment covered areas.

For a particular area, the shape of the ARC is markedly similar for all three frequency bands. The relative total scattering strength, however, does subtly change. R1, R2 and R3 all show the 100kHz data coming in ~ 3-5dB higher, with the 200kHz consistently slightly above the 300 kHz. Areas R4-5-6 in contrast have the 100 kHz ARC steeper thus being slightly lower than the higher frequency results at low grazing angles, switching to higher at high grazing angles.

Comparing Roberts Point and Cordova Channel Results.

It is illuminating to compare and contrast the shape of the ARCs within the three frequency bands for the type localities identified in the BC results. As both data sets were obtained with the identical configuration, even if the data reduction is imperfect, they can be compared in a relative sense. Unfortunately, as the Saipan data were collected from a different platform and calibrated using a different seabed reference, the absolute shape of the curves or level offset cannot be directly compare to the BC results.

From the point of view of this study, the main thing to discern is the extent to which the response curves change with wavelength.

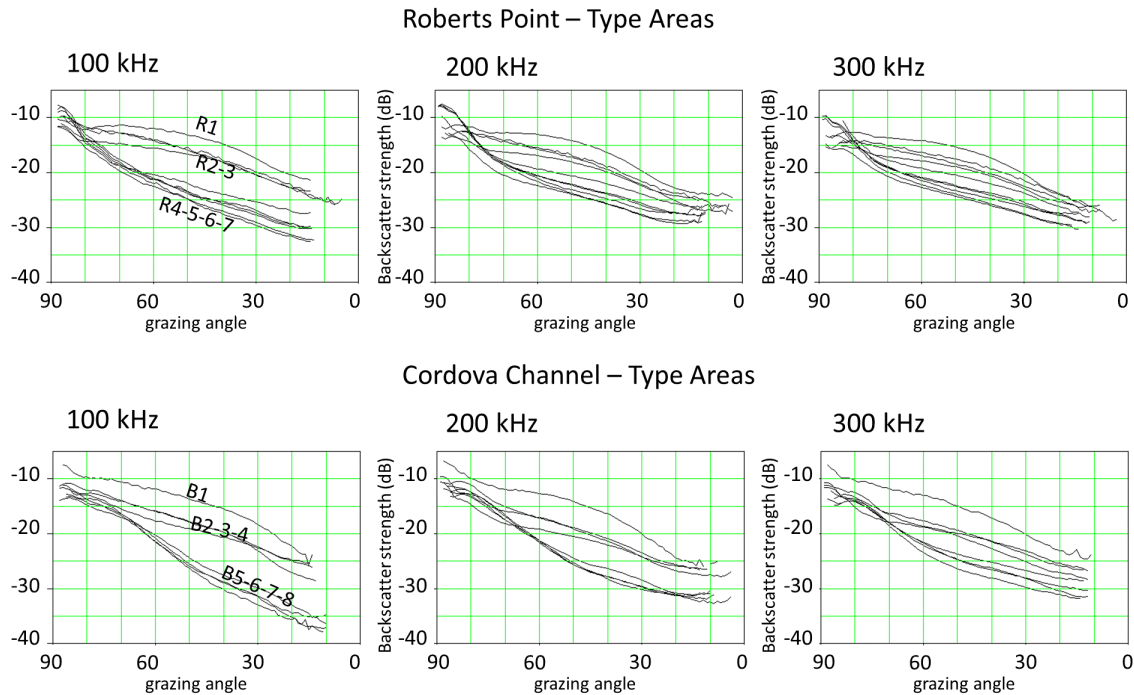


Fig 8: showing the range of backscatter angular response curves from the representative sediment facies observed at the two experimental sites in BC. The curves are compiled by center frequency.

For both areas, at the 100kHz frequency range (Fig. 8 left), the seafloors naturally cluster into three distinctive groups of ARCs.

- R1 and B1 appear very similar and are notably higher in total backscatter strength than all other facies examined.
- R2-3 and B2-3-4 also appear as a distinct cluster.
- The finer grained unconsolidated sediments are quite distinct in both cases but differ between the areas. The Cordova Channel sandy bedforms (B5-6-7-8) show distinctly steeper ARC roll off than those sediments off Roberts Point (R4-5-6-7). The Roberts Point sediments have a more pronounced and narrower near-nadir peak in backscatter.

For the Roberts Point data, as one moves up in frequency to 300 kHz, the clear clustering of the three distinctive facies disappears. At the higher frequency there appears to be a much more continuous and gradual variation in the ARCs. Thus material types that cannot easily be separated at 100 kHz can be divided into subclasses using the higher frequency responses.

For the higher backscatter seabeds, the shape of the low grazing angle roll-off appears invariant between the frequencies, suggesting a rough surface at all wavelengths. In contrast the lower backscatter sediments show a significantly steeper roll off at the lower frequencies suggesting that the roughness with respect to the wavelength is less pronounced at the longer wavelengths.

Coregistration and Textural Complications

At this point, comparisons have primarily been made over length scales of at least half a swath width to extract the full ARC. As one moves to smaller footprint comparisons, one has to address the level of precise coregistration of the imagery. Even though there are sonar mounting offsets, those offsets can be adequately accounted for in the mosaic registration. The exact location of the near nadir peak however, will remain offset, so analysis at dimensions smaller than the instrument offsets could be misleading. This is further compounded by the current necessity to run the survey multiple times as the vessel will never follow exactly the same trajectory.

The main discussion here has been on the use of ARCs to characterize the seafloor. Textural classification that has been used for mono frequency investigations may not be so suited, however, as the minimum spatial dimension of the texture is strongly dependent on the pulse length used. For the case of multi-spectral hardware, the pulse lengths are both different between the frequencies as well as forced to change with range for the highest frequencies.

Conclusions

Through the use of co-mounted multibeam sonars with center frequencies extending over two octaves, the additional discrimination potential of multi-spectral seabed scattering has been investigated. Pronounced changes in spatial patterns visible in geo-referenced mosaicked data are often apparent when the different wavelengths are used. Additionally, the ARCs are seen to diverge significantly in both shape and level as a function of frequency. At this time, without sufficient ground truth data the causes of these changes can only be speculated upon.

The necessary data reduction and calibration steps, already developed for monospectral ARC derivation are compounded herein by having to undertake this for three separate pulse lengths, residual beam patterns and attenuation coefficients. While useful results are herein demonstrated for single deployment data, the complications already present when attempting inter-survey calibrations (Hughes Clarke et al., 2008) will only be compounded three fold.

Grazing angle normalized mosaics can be combined using conventional false colour composite methods to reveal spatial variations in the relative scattering level as a function of frequency. To do so however, requires that the ARC shape variation with grazing angle, and particularly its variation with sediment type, can be estimated and backed out. New approaches which iteratively estimate the local ARC and its spatial variation (e.g. Rzhanov et al., 2012) could overcome this limitation.

As long as the data reduction steps (particularly the residual beam patterns) are managed correctly, the added frequencies could be used to improve ambiguities in inversion for physical properties (e.g. Fonseca and Mayer 2007).

Future Directions

The current proposed approach involves duplication of instrumentation adding additional hardware requirements and commensurate expenses. Transducers than use an even wider band could possibly cover the desired 2 octaves. Notably the R2sonic 2026 apparently can offer usable data outside its optimal 200-400 kHz down to 100 kHz, thus potentially allowing this method to be implemented with no duplication of hardware.

As a general comment, the experimental results noted so far indicate that the lower frequency data tends to provide more contrast. Thus employing even lower frequencies may be of interest. For example the newer EM710 is now supposed to allow data acquisition down to as low as 50 kHz using the same transducers, providing even wider possible wavelength separation.

The choice of frequency range will remain dictated by the depth range of interest. The results presented here chose a range optimized for coastal and continental shelf systems. Other frequency combinations centred at lower frequencies may be equally valid for off shelf operations. For example the RESON 7150 has both 12 and 24kHz available in a single configuration.

For all these systems however, at the moment, they can only be operated within a single frequency band at one time and thus require that lines be repeated. A strongly suggested modification of at least 200-400 kHz sonars would be to allow alternate swaths to sample significantly different parts of the available spectrum thereby avoiding this duplication of shiptime.

Acknowledgements:

This work was supported by an NSERC Discovery Grant to the author. Operational support for the Saipan data was provided by the U.S. Naval Oceanographic Office. OMG sponsorship from Kongsberg Maritime and Rijkswaterstaat covered costs of the BC deployment. Kongsberg Maritime provided technical advice and loan of additional sonar hardware (the 2040C).

References:

- Applied Physics Laboratory, UW, 1994, High-Frequency ocean environmental acoustic models handbook, APL-UW TR 9407-AEAS 9501, Oct. 1994
- Carvalho, R. and Hughes Clarke, J.E., 2012, Proper Environmental Reduction for Attenuation in Multi-sector Sonars , Proceedings of the Canadian Hydrographic Conference, Canadian Hydrographic Association, 15pp.
- de Moustier, C. , 1986, Beyond bathymetry: Mapping acoustic backscattering from the deep seafloor with Sea Beam: Journal of the Acoustical Society of America, Vol. 79, No. 2, p.316-331.
- de Moustier, C. , Alexandrou, D. , 1991, "Angular dependence of 12-kHz seafloor acoustic backscatter", Journal of the Acoustical Society of America, Vol. 90, No. 1, pp. 522 - 531.
- Fonseca, L. and Mayer L., 2007, Remote Estimation of Surficial Seafloor Properties through the Application Angular Range Analysis to Multibeam Sonar Data, Marine Geophysical Researches, v. 28, p.119–126
- Francois R. E., Garrison G. R., 1982a, "Sound absorption based on ocean measurements: Part I: Pure water and magnesium sulfate contributions", Journal of the Acoustical Society of America, 72(3), 896-907.
- Hammerstad, E. (1995, modified in 2000). "EM Technical Note: Backscattering and Seabed Image Reflectivity": Kongsberg Technical Documentation.
- Hughes Clarke, J.E., 1994, Toward remote seafloor classification using the angular response of acoustic backscattering: a case study from multiple overlapping GLORIA data: IEEE Journal of Oceanic Engineering v.19, no.1, p.364-374.

- Hughes Clarke, J.E., Danforth, B.W. and Valentine, P., 1997, Areal Seabed Classification using Backscatter Angular Response at 95 kHz: NATO SACLANTCEN Conference Proceedings Series CP-45, High Frequency Acoustics in Shallow Water, , p.243-250.
- Hughes Clarke, J.E., 2012, Optimal use of multibeam technology in the study of shelf morphodynamics: IAS Special Publication # 44, Sediments, Morphology and Sedimentary Processes on Continental Shelves, p.1-28.
- Hughes Clarke, J.E., Iwanowska, K.K., Parrott, R., Duffy, G., Lamplugh, M. and Griffin, J., 2008, Inter-calibrating multi-source, multi-platform backscatter data sets to assist in compiling regional sediment type maps : Bay of Fundy , Proceedings of the Canadian Hydrographic Conference and National Surveyors Conference, Victoria, BC, Paper 8-2, 22pp.
- Imagenex, 2014, Product Brochure: http://www.imagenex.com/html/rgb_sidescan.html
- Jackson, D.R., Winebrenner, D.P. And Ishimaru, A., 1986, Application of the Composite Roughness Model to High-Frequency Bottom Backscattering: JASA, v.79, p.1410-1422.
- Llewellyn, K, 2005, Corrections for Beam Pattern Residuals in Backscatter Imagery from the Kongsberg-Simrad EM300 Multibeam Echosounder, MScEng Thesis, Dept. Geodesy and Geomatics Engineering, University of New Brunswick.
- NDRC, 1946, Physics of Sound in the Sea, Part II Reverberation, Chapter 15, Shallow Water Reverberation: Division 6, Volume 8 National Defence Research Committee Summary Technical Reports. p.308-323.
- Ogilvy, J.A., 1991, Theory of wave scattering from random rough surfaces, Institute of Physics Publishing, 273 pp.
- Pace, N.G. and Gao, H., 1988, "Swathe Seabed Classification", IEEE Journal of Oceanic Engineering, vol. 13, no. 2, p. 83–90.
- Preston, J., 2009, Automated acoustic seabed classification of multibeam images of Stanton Banks: Applied Acoustics, v.70 (10):11
- Ryan, W.B.F. and Flood, R.D., 1996, Side-looking sonar backscatter response at dual frequencies: Marine Geophysical Researches, v.16 no 6, p.689-705.
- Rzhanov, Y. Fonseca, L., and Mayer, L. A., 2012, Construction of seafloor thematic maps from multibeam acoustic backscatter angular response data: Computers and Geosciences Journal, v.41,. p.181-187.
- Teng, Y.T, 2012, Sector-specific Beam Pattern Compensation for Multi-sector and Multi-swath Multibeam Sonars, MScEng thesis, Dept. Geodesy and Geomatics Engineering, University of New Brunswick.
- Urick, R.J., 1954, The backscattering of Sound from a Harbor Bottom: Journal of the Acoustical Society of America, v.26, no. 2, p.231-235.
- van Zyl, J.J., Burnette, C. F., Farr, T. G., 1991, Inference of surface power spectra from inversion of multifrequency polarimetric radar data: Geophysical Research Letters, v.18, # 9, p.1787-1790.